Pharmacology Research & Perspectives

WILEY | BRITISH PHARMACOLOGICAL SOCIETY

ORIGINAL ARTICLE OPEN ACCESS

β-Caryophyllene Mitigates Thioacetamide-Induced Liver Fibrosis Through CB2-Mediated Suppression of Necroptosis: A Therapeutic Investigation

Lujain Bader Eddin[1] | Seenipandi Arunachalam[1] | Loay Lubbad[2] | Fayez T. Hammad[2] | Ernest Adeghate[3] | Sandeep Subramanya[4] | Shreesh Ojha[1]

[1]Department of Pharmacology and Therapeutics, College of Medicine and Health Sciences, United Arab Emirates University, Al Ain, UAE | [2]Department of Surgery, College of Medicine and Health Sciences, United Arab Emirates University, Al Ain, UAE | [3]Department of Anatomy, College of Medicine and Health Sciences, United Arab Emirates University, Al Ain, UAE | [4]Department of Physiology, College of Medicine and Health Sciences, United Arab Emirates University, Al Ain, UAE

Correspondence: Shreesh Ojha (shreeshojha@uaeu.ac.ae)

Received: 29 April 2026 | **Revised:** 24 June 2026 | **Accepted:** 30 July 2026

Keywords: cannabinoid | Caryophyllene | liver fibrosis | necroptosis | treatment

ABSTRACT

β-Caryophyllene (BCP), a selective agonist of cannabinoid receptor type 2 (CB2), has garnered attention as a promising nutraceutical agent for modulating organ damage. The current study aimed at evaluating the pharmacological role of BCP in Thioacetamide (TAA)-induced liver fibrosis, with particular attention to the involvement of CB2-mediated signaling. Following the induction of fibrosis by TAA, rats were treated with BCP for 6 weeks. In a separate group, AM630, a selective CB2 receptor antagonist, was co-administered with BCP in order to validate CB2-dependent actions. TAA administration triggered significant hepatocellular injury. In addition, TAA activated necroptotic cellular death, shown in the upregulated RIPK1/RIPK3/p-MLKL expression. Growth factors' signaling was disrupted and liver regeneration was impaired. On the contrary, BCP treatment ameliorated oxidative stress, mitigated inflammation, and decreased hepatic stellate cells' activation. This was accompanied by reduced collagen deposition and attenuated fibrosis. BCP markedly abrogated necroptosis and decreased the stimulation of fibrogenic and angiogenic signaling. Additionally, BCP potentiated hepatocytes' survival and restored hepatic regenerative capacity. AM630 co-treatment abolished BCP's protective effects, confirming the CB2 receptors-dependent effects. Given findings highlight BCP as a potential therapeutic agent for liver fibrosis and delineate endocannabinoid system's role in modulating organ fibrosis.

1 | Introduction

Liver is essential in maintaining body's homeostasis, regulating metabolic processes for sugars, proteins, lipids, and detoxifying xenobiotic [1]. Sustained liver injury makes healing injurious and causes the loss of functional hepatic parenchyma, leading to liver fibrosis. Liver fibrosis is characterized by extracellular matrix proteins build-up and the formation of fibrotic scar, with distorted architecture and impaired function [2].

Necroptosis is a regulated form of programmed cell death, involves cell rupture and morphologically marked by the breakdown of the plasma membrane. Its activation depends on various stimuli and requires the action of receptor-interacting serine/threonine kinases 1 and 3 (RIPK1 and RIPK3). Necroptosis is implicated in a variety of liver disorders. TNF signaling is the most prevalent and studied pathway involved in modulating necroptosis. Upon TNF-α binding to TNFR1, the receptor undergoes conformational changes and recruits a group of proteins

forming what is called complex I. The inhibition of cIAPs and the deubiquitination of RIPK1 by CYLD, promote the formation of complex IIb. RIPK1 binds to RIPK3, by intramolecular auto-phosphorylation, where RIPK3 recruits and phosphorylates pseudokinase mixed lineage kinase domain-like (MLKL) to form complex IIc or the necrosome. Phosphorylated MLKL moves to the plasma membrane and oligomerizes, resulting in membrane rupture [3].

Animals fed with a high fat diet (HFD) and Methionine/Choline deficient diet (MCD) had higher hepatic expression of RIPK3, MLKL, and TNF-α associated with induced fibrosis [4]. On the other hand, the deficiency of RIPK3 blunted liver fibrosis associated with MCD diet. The blockage of RIPK1 attenuated features of NASH in mice and reduced steatosis [5]. In addition, Choline-deficient L-amino-defined (CDAA) diet-induced fibrosis was reduced in mice lacking RIPK3. CDAA-fed mice produced hepatic nodules, which were diminished in RIPK3 knockout mice [6].

Hepatotoxic molecules can interact with cellular components, leading to liver lesions. The hepatotoxic effects of thioacetamide (TAA) resemble pathological features of liver fibrosis. Preclinical studies showed a close resemblance of TAA-induced liver fibrosis with human liver pathology [7, 8]. TAA-induced hepatotoxicity is a favorable model due to its high specificity in liver targeting. TAA initiates its toxic effects following its bioactivation by cytochrome P2E1 and flavin adenine dinucleotide monooxygenase, and the generation of reactive metabolites [9].

β-Caryophyllene is a naturally occurring bicyclic sesquiterpene abundantly present in the essential oils of numerous aromatic plants, including black pepper (*Piper nigrum*), cloves (*Syzygium aromaticum*), and cannabis (*Cannabis sativa*). Its spicy, woody, and peppery aroma encouraged its broad utilization in food industries and fragrance formulations [10]. BCP modulates the endocannabinoid system by selectively binding and activating CB2 cannabinoid receptors, a unique property of BCP unlike other dietary terpenes. CB2 receptors' activation contributes to its immunomodulatory actions devoid of psychoactive effects associated with CB1 receptors' activation [11]. BCP exerts an anti-inflammatory effect through the suppression of pro-inflammatory cytokines' release. This effect has been demonstrated in conditions such as arthritis, colitis, and neuroinflammatory diseases. It has also a potent antioxidant activity through neutralizing free radicals and reducing oxidative stress [12]. This contributes to its protective effects against various inflammatory conditions including fibrosis [13].

As inflammation is a key mediator of liver fibrosis, in this study, we investigated BCP's beneficial effects against TAA-induced fibrosis and whether these effects are CB2 receptors dependent.

2 | Materials and Methods

2.1 | Chemicals

Thioacetamide and β-Caryophyllene were obtained from Thermo Fisher Scientific (Ward Hill, MA, USA) and Sigma-Aldrich (St. Louis, MO, USA), respectively. AM630 was sourced from GLPBIO (Cat. No. GC10147). All compounds were freshly prepared each day prior to administration. Thioacetamide was dissolved in distilled water, while β-Caryophyllene (BCP) was diluted in scientific-grade light olive oil. AM630 was initially mixed with 2 mL of dimethyl sulfoxide (DMSO) and 200 μL of Tween-80, and then diluted in normal saline for final preparation.

2.2 | Experimental Animals

Six-week-old male albino Wistar rats (180–240 g) were obtained from the UAE University's animal research facility. They were housed under standard conditions with free access to food and water on a 12-h light/dark cycle. Animals were acclimated for 1 week before treatment. All procedures were approved by the university's Animal Ethics Committee (No. ERA_2025_5826).

2.3 | Experimental Protocol

In this approach, rats were categorized into 4 groups (10 rats for each). Treatment was given as illustrated in Figure 1. Group 1 (Control; CON) received normal saline intraperitoneally for 8 weeks. Group 2 (Thioacetamide; TAA) received 200 mg/kg of TAA intraperitoneally thrice a week for 8 weeks. Group 3 (β-caryophyllene and Thioacetamide; BCP + TAA) received TAA from Week 1 to Week 6; BCP started on Week 6 with an oral daily dose of 50 mg/kg BCP followed by TAA administration in 1-h intervals. The dose of BCP is based on previous studies showing a significant effect exerted at the range of 30–100 mg/kg. A dose of 50 mg/kg was shown to produce pharmacological, behavioral, and biological effects without observed toxicity at a mid-range selected dose [14, 15]. A single dose was selected as the aim of the study is to investigate mechanistic pathways. A single dose approach has been applied in proof-of-concept studies evaluating biological response at a specific exposure level. This is acceptable as long as the biological effectiveness of the dose has been identified in the literature. Group 4 (AM630 + BCP + TAA) received a daily intraperitoneal injection of AM630 (2.5 mg/kg), 1 h before BCP dose, starting at Week 6.

2.4 | Tissue Collection

At the end of the experimental treatment, rats were decapitated and blood was collected into tubes without anticoagulant. Livers were excised, rinsed with phosphate-buffered saline, and sectioned. Portions were snap-frozen in liquid nitrogen and stored at −80°C for later analysis. Other sections were fixed in 4% formalin, processed, and preserved in paraffin blocks.

2.5 | Protein Extraction

Liver samples were homogenized in RIPA buffer (Millipore, Burlington, MA, USA) with added phosphatase and protease inhibitors (Thermo Fisher Scientific, Cat No. 78440) using a tissue homogenizer. Homogenates were centrifuged at 15 000 × g for

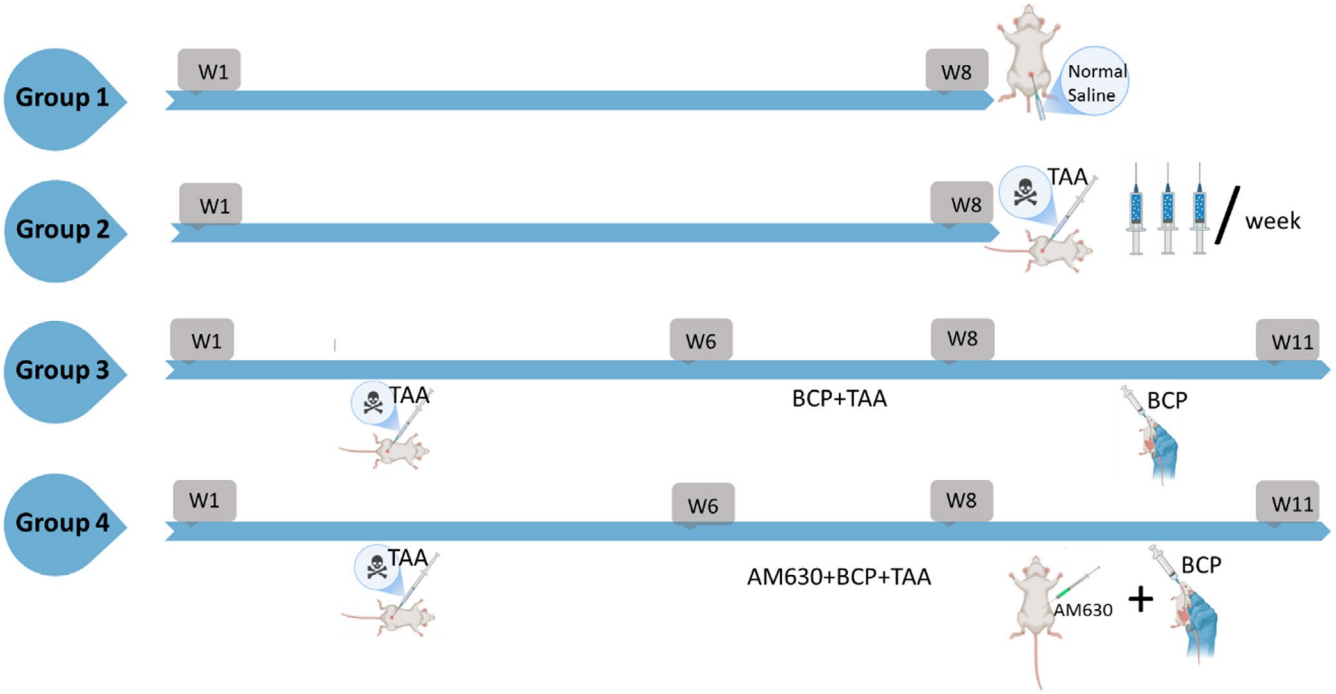

FIGURE 1 | Experimental study design.

30 min at 4°C, and the supernatants were collected and stored at −40°C for further analyses.

2.6 | Liver Index

Rats' body weight was recorded weekly. Rats' liver weight was recorded at the last week of the experiment on the sacrifice day. Liver index was calculated by taking the ratio of the liver weight to body weight for each rat in all groups.

2.7 | Functional Parameters

The level of Aspartate aminotransferase (AST) and Alanine aminotransferase (ALT) was measured in serum using commercial kits purchased from MyBioSource (Southern California, San Diego, USA, Cat No. MBS264975, MBS269614, respectively).

2.8 | Hydroxyproline Assay

Total hydroxyproline was measured using a commercial kit obtained from Cayman (Michigan, USA, Cat No. 702440) by following the inserted protocol. The assay was performed in serum samples.

2.9 | Matrix Metalloproteinase-2 and 9 (MMP2 and MMP9) Assay

The level of both MMP2 and MMP9 enzymes in serum was determined by a colorimetric assay of an ELISA approach using biochemical readily supplied kits from R&D (Minneapolis, USA, Cat No. MMP200, DY8174-05, respectively).

2.10 | Picrosirius Red Staining

Sections of 3 μm thickness of paraffin embedded fixed livers were prepared on slides and deparaffinized. Picrosirius red staining was performed as per manufacturer's protocol (Abcam, Cambridge, UK, Cat No. ab245887). Stained sections were viewed under light microscope (Olympus, Hamburg, Germany).

2.11 | Oil Red O Staining

Frozen sections of 6 μm thickness were cryo-sectioned and prepared on slides. Oil Red O Staining was performed as per manufacturer's protocol (Abcam, Cambridge, UK, Cat No. ab150678). Stained sections were viewed under a light microscope (Olympus, Hamburg, Germany).

2.12 | Immunohistochemical Staining

Paraffin-embedded tissue sections were processed using the avidin-biotin-peroxidase technique and developed with 3,3′-diaminobenzidine (DAB). Antigen retrieval was performed through dewaxing followed by immersion in citrate buffer. Primary antibodies (listed in Table 1) were applied, and the sections were incubated overnight. Subsequently, biotinylated secondary antibodies targeting mouse and rabbit IgG (dilution 1:100) were applied. The avidin-biotin complex (Vectastain Elite ABC kit) was then added and incubated

TABLE 1 | Primary antibodies used in immuno-staining, with their dilution ratio and source.

Antibody	Dilution ratio	Company and catalog number
Fibronectin	1:50	Santa Cruz Biotechnology (sc-8422)
COL3A1	1:100	Santa Cruz Biotechnology (sc-271249)
α-SMA	1:50	Cell Signaling Technology (14968s)
F4/80	1:100	Santa Cruz Biotechnology (sc-377009)
CD68	1:100	Santa Cruz Biotechnology (sc-20060)

TABLE 2 | Primary antibodies used in Western blotting, with their dilution ratio and source.

Antibody	Dilution ratio	Company and catalog number
RIPK1	1:500	Santa Cruz Biotechnology (sc-8422)
RIPK3	1:500	Santa Cruz Biotechnology (sc-52751)
p-MLKL	1:500	Cell Signaling Technology (14968s)
PDGF	1:1000	Santa Cruz Biotechnology (sc-9974)
VEGF	1:1000	Santa Cruz Biotechnology (sc-7269)
HGF-α	1:1000	Santa Cruz Biotechnology (sc-374422)
NOX2	1:500	Thermo Fisher Scientific (MA5-35348)
GPX4	1:1000	Santa Cruz Biotechnology (sc-166570)
GAPDH	1:1000	Santa Cruz Biotechnology (sc-32233)

for 1 h. Visualization was achieved using the DAB substrate (Vector Laboratories Inc., Burlingame, CA, USA). Finally, the stained sections were mounted with DPX medium and examined under a light microscope (Olympus, Hamburg, Germany). Quantitative analysis of staining intensity was performed using ImageJ software (National Institutes of Health, Bethesda, MD, USA).

2.13 | Western Blotting Assay

The protein concentration in homogenized liver tissue samples was determined using the Pierce BCA Protein Assay Kit (Thermo Fisher Scientific, Rockford, IL, USA, Ca No. 23227). Equal amounts of extracted protein samples were mixed with RIPA buffer (Thermo Fisher Scientific, Rockford, IL, USA, Ca No. 89901) and Laemmli buffer (Bio-Rad, Hercules, CA, USA, Ca No. 1610747) containing 2-mercaptoethanol (Sigma-Aldrich, St. Louis, MO, USA, Ca No. 805740). The samples were then heated at 95°C for 5 min to achieve protein denaturation and stored for further analysis. Proteins were separated by SDS-PAGE and transferred onto PVDF membranes. The membranes were blocked with 5% bovine serum albumin (BSA) for 1 h to prevent nonspecific binding. Following blocking, membranes were incubated overnight with primary antibodies listed in Table 2. Detection was performed using horseradish peroxidase (HRP)-conjugated secondary antibodies (Cell Signaling Technology, Anti-rabbit IgG, Ca No. 7074, Anti-mouse IgG, Ca No. 7076) specific to mouse and rabbit originated antibodies and enhanced chemiluminescence substrate (Thermo Fisher Scientific, Waltham, MA, USA, Ca No. 34580). Band intensities were quantified using ImageJ software (National Institutes of Health, Bethesda, MD, USA). Glyceraldehyde-3-phosphate dehydrogenase (GAPDH) was used as a loading control to normalize total protein expression levels.

2.14 | Gene Expression Analysis

RNA was extracted from frozen liver samples following the manufacturer's protocol of Qiazol Lysis reagent (Qiagen, Hilden, Germany). Tissues were homogenized using a zirconium beads mix of 0.5 mm and 3 mm sizes on a bead homogenizer. Quality and quantity of extracted RNA samples were determined on a NanoDrop 2000 Spectrophotometer (Thermo Fisher Scientific Inc., Wilmington, DE, USA). 1 μg of extracted RNA samples was converted to cDNA following the manufacturer's protocol of QuantiTect reverse transcription kit (Qiagen, Hilden, Germany). Gene expression analysis was carried out utilizing probe hydrolysis real-time PCR chemistry on a Quantstudio 7 instrument (Thermo Fisher Scientific Inc., Wilmington, DE, USA), as a housekeeping gene, Peptidylprolyl Isomerase A (PPIA) was used as a reference for normalization. PPIA probe was Quasar 670-labeled while other target genes' probes were FAM-labeled. Relative gene expression quantification was calculated using the delta–delta CT (ΔΔCT) method. Sequences of primers and probes are included in Table 3.

2.15 | Statistical Analysis

Date were derived from independent biological replicates, representing different rats. Data were expressed as the mean ± standard error of the mean (SEM). Statistical comparisons between groups were conducted using one-way analysis of variance (ANOVA), followed by Duncan's Multiple Range Test (DMRT) for post hoc analysis. All statistical analyses were performed using SPSS software. A p-value ≤ 0.05 was considered statistically significant. Although the statistical approach employed in the present study was appropriate for the experimental design and enabled identification of significant differences among groups, future investigations may benefit from complementary analyses using more conservative post hoc tests to provide

TABLE 3 | Primers and fluorogenic probe sequences used in real-time PCR.

TNF-α (NM_012675.3)	Forward CTCACACTCAGATCATCTTCTC
	Reverse CCGCTTGGTGGTTTGCTAC
	Probe FAM-CTCGAGTGACAAGCCCGTAGCC-BHQ-1
IL-6 (NM_012589.2)	Forward TCACAGAGGATACCACCCACAACA
	Reverse CACAAGTCCGGAGAGGAGAC
	Probe FAM-TCAGAATTGCCATTGCACAACTCT-BHQ-1
IL-1β (NM_031512.2)	Forward ATGCCTCGTGCTGTCTGACC
	Reverse GCTCATGGAGAATACCACTTGTTGG
	Probe FAM-AGCTGAAAGCTCTCCACCTCAATGGA-BHQ-1
TGF-β1 NM_012620.1	Forward GTGGCTGAACCAAGGAGACG
	Reverse CGTGGAGTACATTATCTTTGCTGTC
	Probe FAM-ACAGGGCTTTCGCTTCAGTGCTC-BHQ—
MCP-1 (NM_031530.1)	Forward GCTGTCTCAGCCAGATGCAG
	Reverse CCAGCCGACTCATTGGGA
	Probe FAM-CCCACTCACCTGCTGCTACTCA-BHQ-1
COLA-1 (NM_053304.1)	Forward CTGACTGGAAGAGCGGAGAGT
	Reverse CCTGTCTCCATGTTGCAGTAGAC
	Probe FAM-ACTGGATCGACCCTAACCAAGGC-BHQ-1
GPX1 (NM_030826.4)	Forward GTGCTGCTCATTGAGAATGTCG
	Reverse TCATTCTTGCCATTCTCCTGATG
	Probe FAM-TCCCTCTGAGGCACCACGAC-BHQ-1
PPIA (NM_017101.1)	Forward GCGTCTGCTTCGAGCTGT
	Reverse CACCCTGGCACATGAATCC

additional confirmation of the observed treatment effects and strengthen the statistical robustness.

3 | Results

3.1 | Liver Morphology and Injury Markers

As depicted in (Figure 2A), the liver gross morphology of CON rats shows a smooth reddish surface. However, TAA exposure induced an irregular shape with widespread micro- and macro-nodules. Treatment with BCP prevented the formation of macro-nodules with a nearly normal external surface and minimal micro-nodules appearance. Administration of the AM630 compound caused a similar effect to what was observed in TAA-injected rats with a coarse surface and clearly formed nodules.

The relative liver weight in the TAA group was increased significantly compared to the CON group. BCP treatment significantly prevented the increase in the relative liver index induced by TAA. In a similar manner to TAA, AM630 administration caused an upsurge in the liver/body ratio in the AM630 + BCP + TAA group when compared to the BCP + TAA group (Figure 2B).

Both ALT and AST enzyme activities were evaluated in liver fibrotic injury. ALT and AST serum levels were significantly elevated in TAA group, reflecting impaired liver function. Post-treatment with BCP diminished ALT and AST levels. AM630 injection before BCP treatment resulted in a reversed effect on hepatic functional enzymes shown by elevated levels of both ALT and AST (Figure 2C,D).

3.2 | Hepatic Fibrosis, Extracellular Matrix Remodeling and Lipid Accumulation

The accumulation of collagen was evaluated by Pirosirius Red staining. As shown in (Figure 3A) chronic administration of TAA increased hepatic collagen expression when compared to CON sections. However, BCP treatment attenuated the effect of TAA on fibrosis progression. The figure also shows the inhibitory effect of AM630 on BCP protective effects, where increased collagen expression was observed.

Lipid accumulation was assessed using Oil Red O staining. CON group showed minimal lipid droplets deposition and normal architecture. Whereas, TAA group showed a significant increase

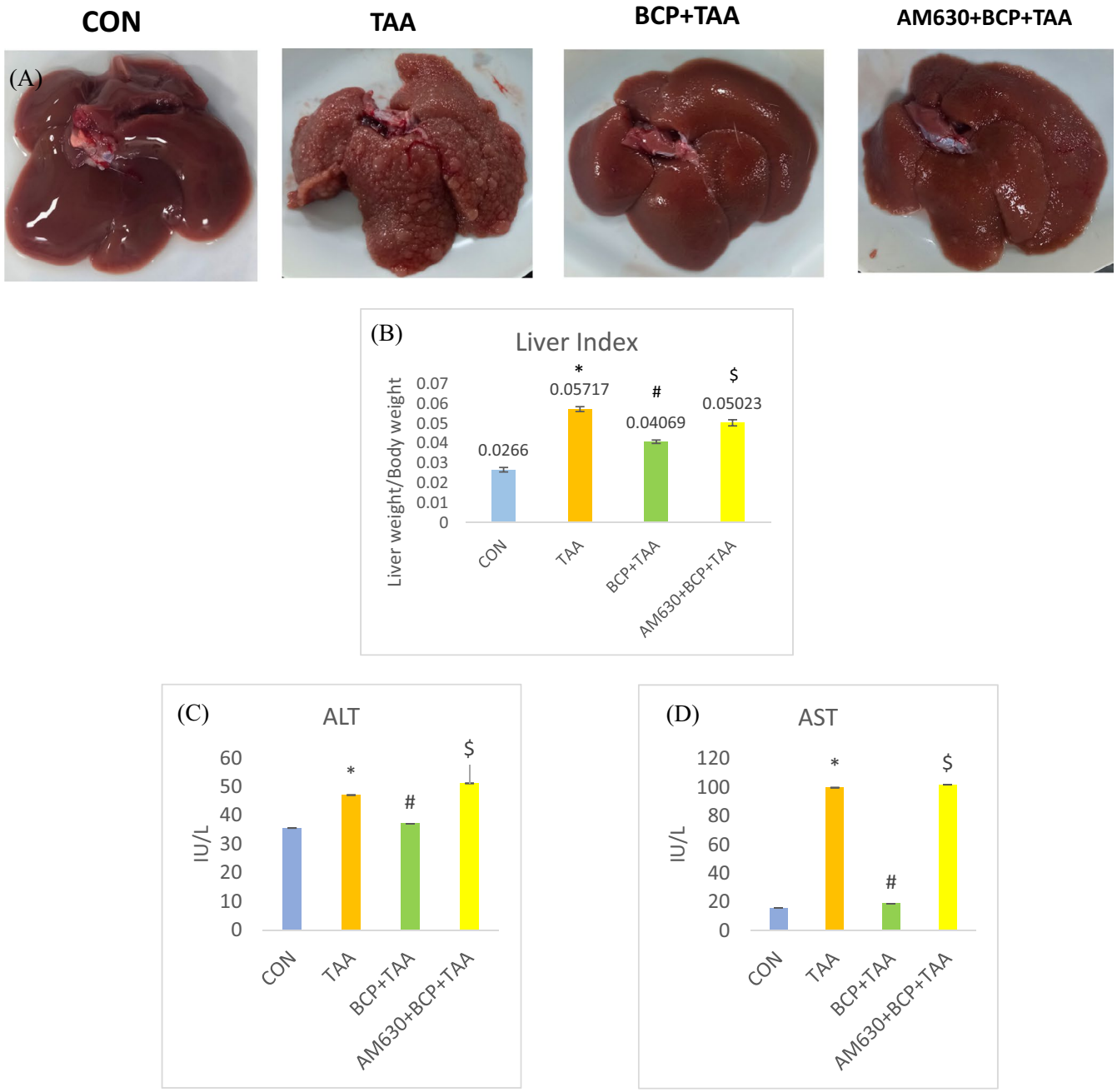

FIGURE 2 | (A) Liver images. (B) Liver index among different groups. Level of (C) ALT and (D) AST markers in serum ($n = 7–8$) $^{*}p < 0.05$ CON vs. TAA, $^{\#}p < 0.05$ TAA vs. BCP + TAA, $^{\$}p < 0.05$ BCP + TAA vs. AM630 + BCP + TAA (one-way ANOVA followed by DMRT). CON: Control, BCP + TAA: β-Caryophyllene+ Thioacetamide treatment, AM630 + BCP + TAA: AM630 + β-Caryophyllene+ Thioacetamide.

in intracellular lipid accumulation manifested by the abundant red-stained lipid droplets. BCP treatment ameliorated TAA-induced steatotic change and reduced lipid deposition, as shown by the less stained lipid droplets. Co-administration of AM630 reverted the steatotic profile to an expression pattern similar to the TAA group (Figure 3B).

Hydroxyproline is a biomarker for collagen turnover used to assess fibrosis severity. TAA injections caused a considerable elevation in hydroxyproline level compared to CON group values. BCP-treated rats had a significant decrease in serum level of hydroxyproline when compared to the TAA group. Moreover, AM630 pre-administration blocked BCP-mediated decrease in hydroxyproline as illustrated in Figure 3C.

Extracellular matrix degradation was assessed by measuring the level of MMP2 and MMP9 enzymes in liver tissue (Figure 3D,E). The level of both enzymes was increased in the TAA group compared to the CON group. However, BCP treatment showed a reduced observed level in both MMP2 and MMP9. AM630 administration prior to BCP resulted in an elevated enzyme level compared to the BCP + TAA group.

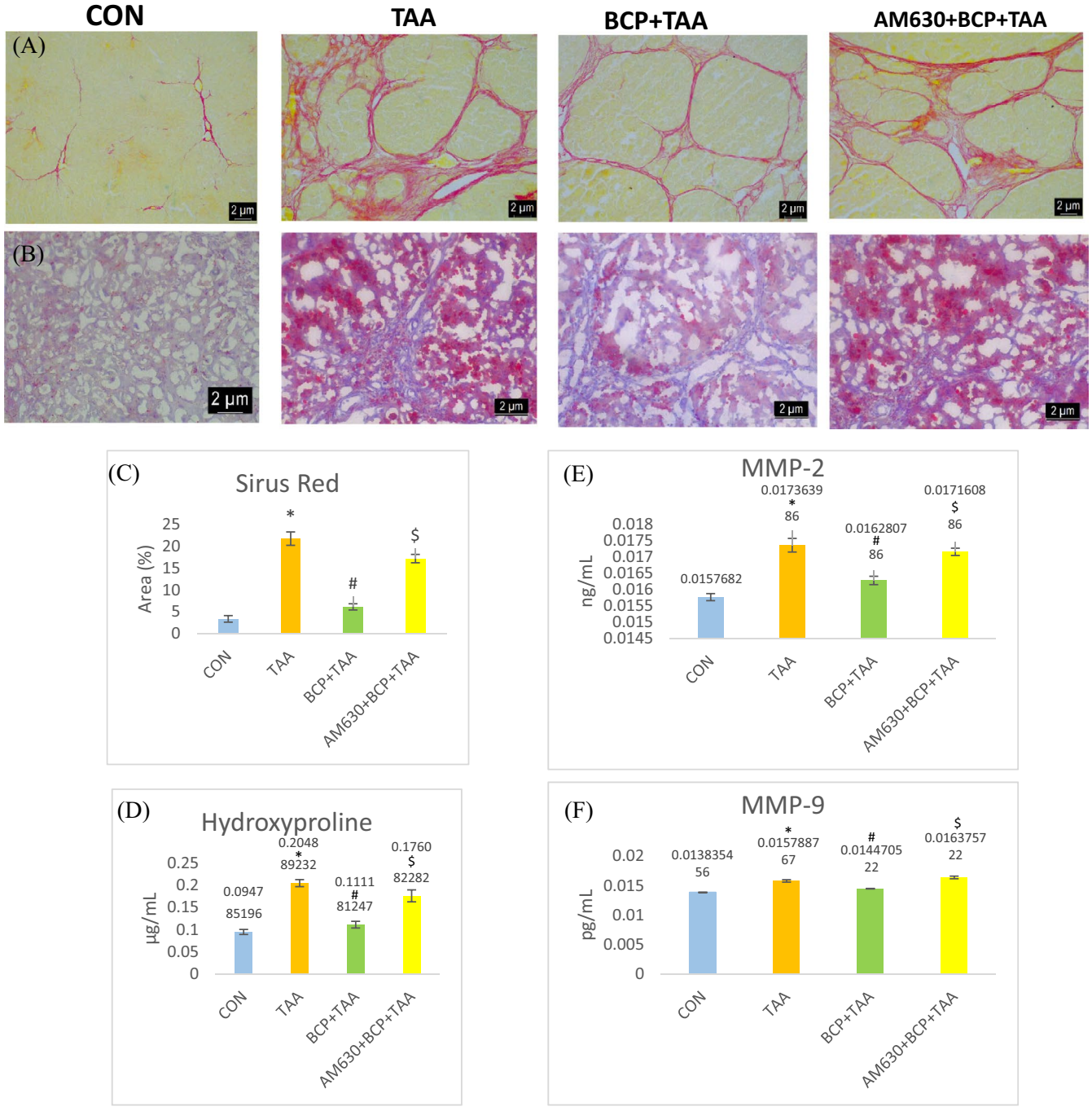

FIGURE 3 | (A) Pirosirius Red liver staining. (B) Oil Red O staining. (C) Quantification of Pirosirius Red staining. (D) Hydroxyproline level in serum. Enzyme level of (E) MMP2 and (F) MMP9 ($n = 7–8$) in liver tissue. $^{*}p < 0.05$ CON vs. TAA, $^{\#}p < 0.05$ TAA vs. BCP + TAA, $^{\$}p < 0.05$ BCP + TAA vs. AM630 + BCP + TAA (one-way ANOVA followed by DMRT). CON: Control, BCP + TAA: β-Caryophyllene+ Thioacetamide treatment, AM630 + BCP + TAA: AM630+ β-Caryophyllene+ Thioacetamide.

3.3 | Immunohistochemical Staining of Liver Tissue

Immunohistochemical staining was performed to assess the effect of TAA on fibrosis and macrophage activation. The staining analysis demonstrated an altered deposition of ECM, HSC activation, and macrophage infiltration in the TAA group. There was a profound increase in COL3A1 and fibronectin, which indicates progressive fibrotic remodeling (Figure 4A,B). In addition, periportal and perisinusoidal regions showed intense staining of α-SMA, a marker of activated HSC (Figure 4C). TAA administration also induced remarkable macrophage infiltration, evident in the increased $CD68^{+}$ and $F4/80^{+}$ immunoreactivity (Figure 4D,E). BCP treatment significantly attenuated TAA-induced alterations. BCP-treated rats exhibited reduced COL3A1, fibronectin, and α-SMA expression, with decreased $CD68^{+}$ and $F4/80^{+}$ immunoreactivity. AM630 reversed the antifibrotic and anti-inflammatory effects of BCP, restoring the

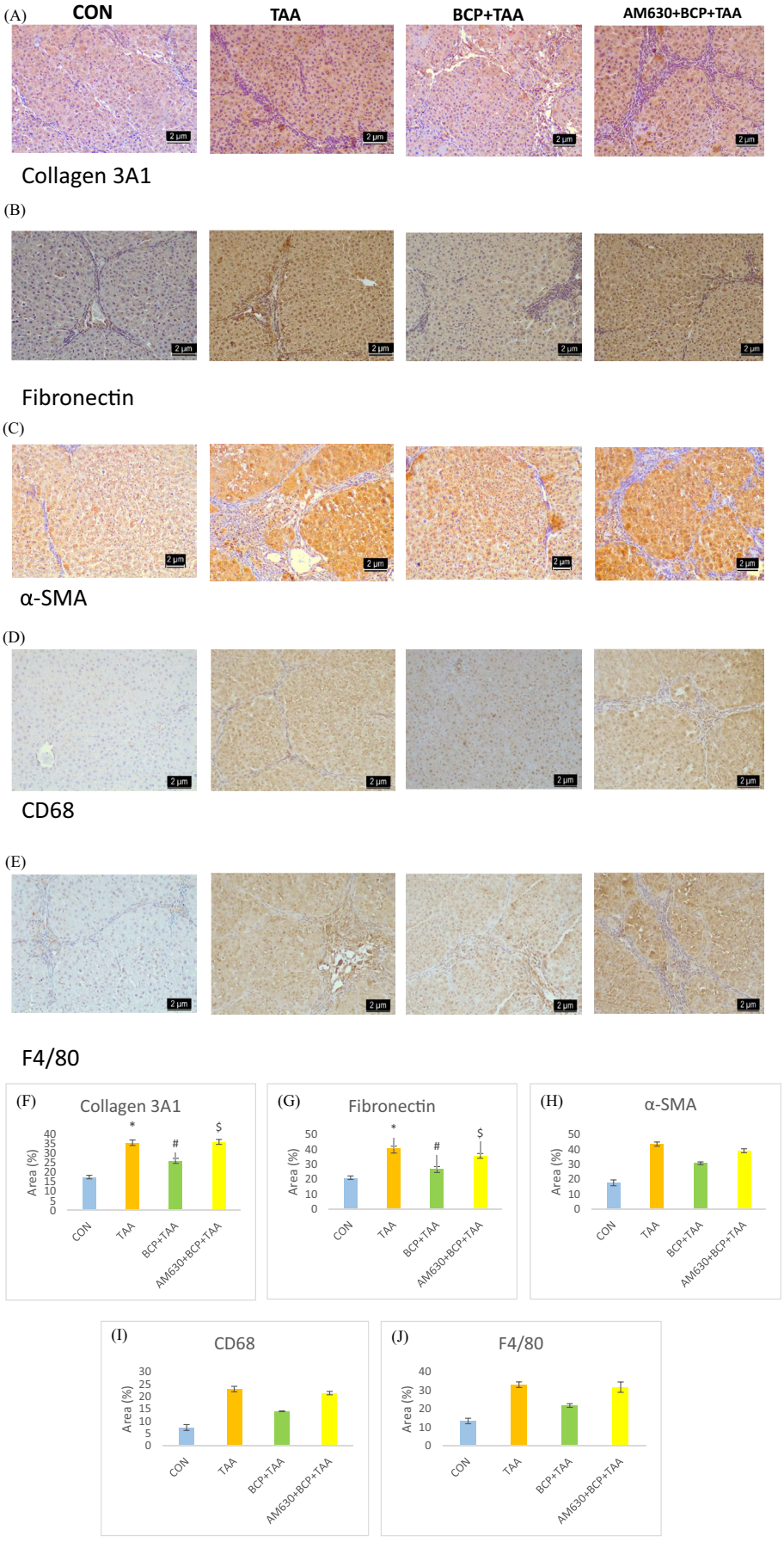

FIGURE 4 | Legend on next page.

FIGURE 4 | Immunohistochemical staining of (A) COL3A1, (B) Fibronectin, (C) α-SMA, (D) $CD68^+$ and (E) $F4/80^+$. (F–J) Quantification of the corresponding markers. Scale bar = 2 μm. CON: Control, BCP + TAA: β-Caryophyllene+ Thioacetamide treatment, AM630 + BCP + TAA: AM630 + β-Caryophyllene + Thioacetamide.

expression of fibrotic and inflammatory markers similar to the TAA group.

3.4 | Fibrotic, Inflammatory and Oxidative Genes Expression

Real-time PCR was utilized to identify the level of gene expression of fibrotic, inflammatory, and oxidative markers. Compared to the CON group, Col-1 and TGF-β gene expression was significantly increased in TAA-injected rats, whereas with BCP treatment, a decreased expression was observed. As shown in the AM630 + BCP + TAA group, AM630 abolished the antifibrotic effect of BCP (Figure 5A,B).

In line with the above observation, gene expression of inflammatory markers that include Interleukin-1β (IL-1β), Interleukin-6 (IL-6), Monocyte Chemotactic Protein 1 (MCP-1), and Tumor Necrosis Factor alpha (TNF-α) followed the same pattern of expression as the fibrotic genes in each corresponding group. An upregulated expression of the four markers was observed in the TAA group compared to the CON group, an effect that was mitigated by BCP treatment (Figure 5C–F).

In addition, the gene expression of glutathione peroxidase 1 (GPX1), an antioxidant marker, showed a striking decrease in TAA-injected rats and this effect was ameliorated by BCP treatment (Figure 5G).

3.5 | Effect of BCP on Necroptosis Induction

Figure 6 shows the western blot analysis of necroptosis markers that include RIPK1, RIPK3 and p-MLKL. The TAA group showed a significant increase in the protein expression of the three markers. Notably, BCP-treated group showed a significant decrease in RIPK1, RIPK3 and MLKL protein expression compared to TAA group. AM630 + BCP + TAA group showed an induced expression of necroptosis proteins compared to BCP + TAA group.

3.6 | Effect of BCP on Pro- and Anti-Fibrogenic Growth Factors Protein Expression

Platelet-derived growth factor (PDGF) and Vascular Endothelial Growth Factor (VEGF) are fibrogenesis-associated proteins that promote activation of hepatic stellate cells. The protein expression of both VEGF and PDGF was determined by western blotting analysis (Figure 7A). In TAA-injected rats, TAA resulted in a significant upregulated expression of VEGF and PDGF. BCP treatment in TAA-injected rats reinstated the expression of VEGF and PDGF to a comparable normal level when compared to the TAA group. The level of VEGF and PDGF was significantly increased in the AM630 + BCP + TAA group.

Hepatocyte growth factor-α (HGF-α) expression reflects liver's capability to wound heal and regenerate itself. TAA induction resulted in a marked decrease in HGF-α expression compared to the CON group, whereas BCP treatment significantly restored HGF-α to near-normal levels and potentiated liver's regenerative ability. The co-administration of MA630 with BCP abolished BCP effects and decreased HGF-α expression to values comparable to the TAA group (Figure 7B).

3.7 | Effect of BCP on Oxidative Markers Expression

Disrupted antioxidant defense contributes significantly to fibrotic injury. TAA administration resulted in a marked reduction in GPX4 expression with concomitant elevation in NOX2 level compared to CON group. In contrast, BCP-treated rats showed a restoration of a balanced antioxidant defense. BCP restored GPX4 expression and resulted in an accompanied decrease in NOX2. Co-administration of AM630 with BCP inhibited BCP effects and maintained an expression level similar to what was observed in TAA group (Figure 8).

4 | Discussion

This study investigated the therapeutic effects of BCP on an experimental model of liver fibrosis induced by intraperitoneal administration of TAA. In order to evaluate the therapeutic rather than preventive potential of BCP, treatment was initiated after 6 weeks of TAA administration, a time point at which hepatic fibrosis is known to be established. Our findings demonstrated that BCP markedly attenuated TAA-induced liver damage, as evidenced by improvements in liver function markers, histopathological architecture, inflammatory mediators, oxidative stress parameters, and fibrosis-associated markers. Furthermore, the antifibrotic effects of BCP were attenuated by co-administration of the CB2 receptor antagonist AM630, indicating that CB2 receptor activation contributes to the observed effects of BCP.

Elevated aminotransferase enzyme levels are a reflection of liver damage. Our results showed that TAA significantly elevated serum ALT and AST levels, which is consistent with the results reported by other researchers [16]. In contrast, BCP effectively mitigated the rise and restored enzyme levels toward normal values as previously documented [17]. Moreover, BCP reduced the liver index, which has been elevated following TAA administration, supported by earlier studies [18].

Activation of hepatic stellate cells (HSC) is considered the cornerstone in the induction of hepatic fibrosis [19]. TGF-β is a regulator of fibrogenesis, acting primarily through its receptors on HSC to induce their activation. Once activated, HSCs express several markers that are typically absent in quiescent cells, such as α-SMA [20]. In our study, immunostaining

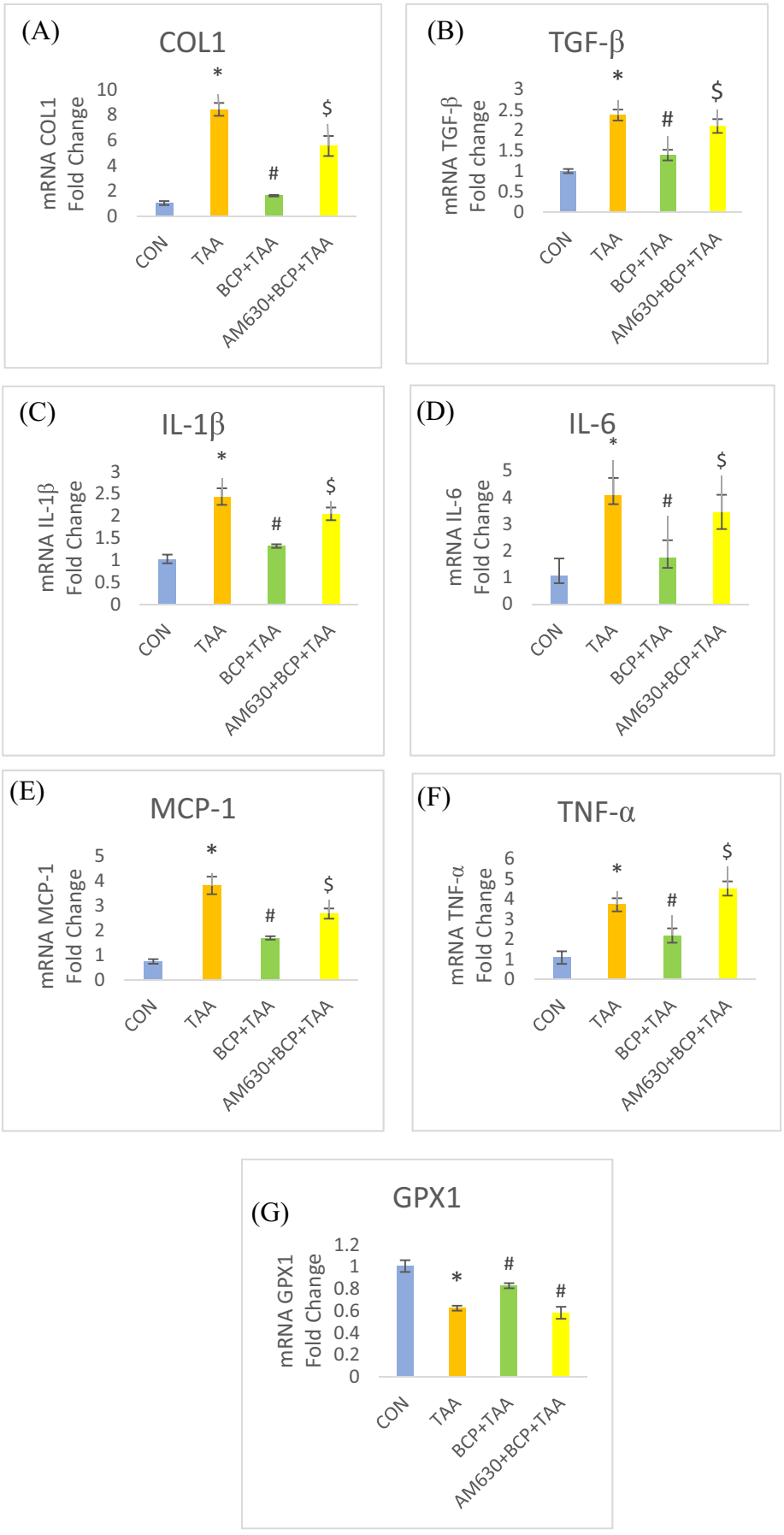

FIGURE 5 | Legend on next page.

FIGURE 5 | Gene expression of fibrotic, inflammatory and oxidative markers. (A) Col-1, (B) TGF-β, (C) IL-1β, (D) IL-6, (E) MCP-1, (F) TNF-α, (G) GPX1. *$p < 0.05$ CON vs. TAA, #$p < 0.05$ TAA vs. BCP + TAA, $$p < 0.05$ BCP + TAA vs. AM630 + BCP + TAA (one-way ANOVA followed by DMRT). CON: Control, BCP + TAA: β-Caryophyllene+ Thioacetamide treatment, AM630 + BCP + TAA: AM630 + β-Caryophyllene+ Thioacetamide.

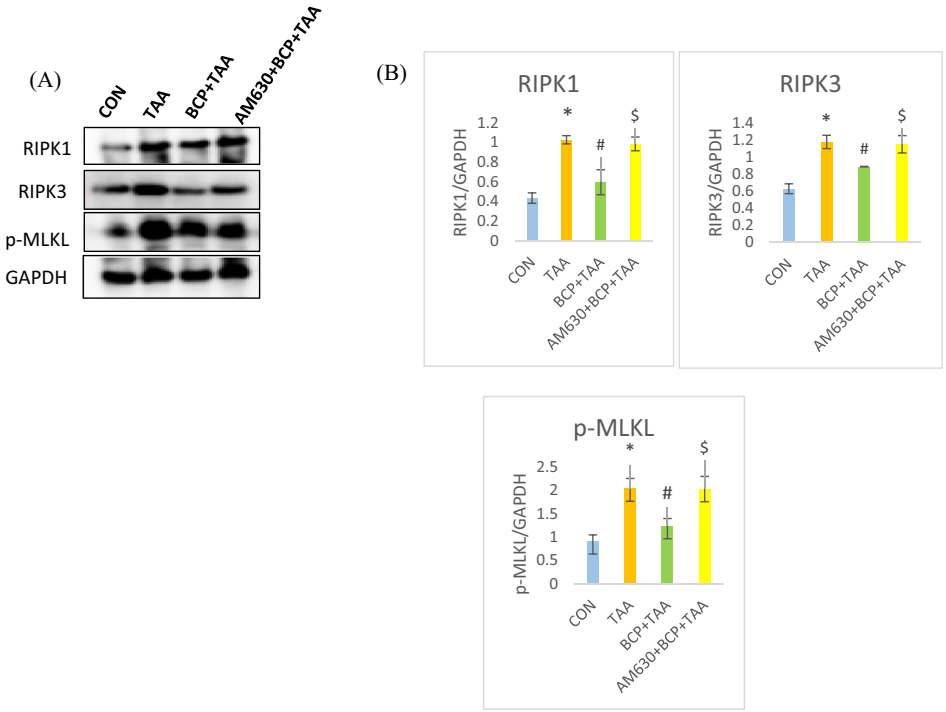

FIGURE 6 | Protein expression of necroptosis markers; RIPK1, RIPK3 and p-MLKL. (A) Immunoblotting analysis of RIPK1, RIPK3 and p-MLKL. (B) Quantification of RIPK1, RIPK3 and p-MLKL protein expression ($n = 3–4$). *$p < 0.05$ CON vs. TAA, #$p < 0.05$ TAA vs. BCP + TAA, $$p < 0.05$ BCP + TAA vs. AM630 + BCP + TAA (one-way ANOVA followed by DMRT). CON: Control, BCP + TAA: β-Caryophyllene+ Thioacetamide treatment, AM630 + BCP + TAA: AM630 + β-Caryophyllene + Thioacetamide.

revealed an increased expression of both TGF-β and α-SMA in the TAA-injected group, consistent with previous reports [21]. Activated HSC subsequently promotes excessive synthesis of extracellular matrix proteins, including collagen and fibronectin. In addition, the gene expression of both collagen and fibronectin was significantly upregulated in the TAA group. Sirius Red staining also confirmed the buildup of collagen in TAA liver sections. In agreement with earlier studies, BCP treatment ameliorated these histopathological changes induced by TAA [22–24]. Moreover, hydroxyproline, an essential amino acid in collagen, has been evaluated as a marker of collagen accumulation and fibrosis development. The levels of hydroxyproline were significantly elevated in the TAA group compared with the CON group, which corroborates the development of fibrosis in TAA-injected rats. This is similar to what is documented earlier showing that fibrosis is correlated with an elevated hydroxyproline level [25]. However, the BCP-treated group showed a marked reduction in hydroxyproline. The effect of BCP on hydroxyproline content has not been previously described; our findings introduce new evidence supporting its antifibrotic potential.

Chronic inflammation is a central pathogenic mechanism in liver fibrogenesis. Persistent inflammatory signaling deteriorates tissue damage and promotes wound healing response and fibrotic scar formation. TAA stimulates an inflammatory injury due to its induced oxidative damage and cellular demise [26]. Rats treated with TAA showed significantly elevated gene expression of inflammatory cytokines, IL-1β, IL-6, MCP-1, and TNF-α, in parallel with previous studies [27]. In contrast, BCP-treated rats exhibited a remarkable decrease in their expression. Our findings are consistent with the reported anti-inflammatory effect of BCP in experimental liver fibrosis [22, 24]. Immunohistochemical staining showed a profound increase in the infiltrated macrophages in TAA-injected rats, indicating an active recruitment and activation of immune cells within periportal and parenchymal regions of the liver. BCP treatment was correlated with diminished expression of $CD68^+$ and $F4/80^+$ cells. Our data align closely with previous reports about the anti-inflammatory effect of BCP [17], and also remain consistent with other reports for the protective effects of herbal constituents in TAA-induced liver injury [28].

TAA is a well-established inducer of hepatic fibrosis. The reactive metabolites of TAA interact with cellular components causing the generation of highly reactive free radicals. Oxidative stress drives an acute inflammatory reaction that progresses to hepatocellular damage [29, 30]. This injury is associated with dysregulated redox balance, characterized by reduced activity of the anti-oxidant enzymes GPX1 and GPX4, along with potentiated NOX2-mediated ROS generation. Study outcomes showed that treating TAA-induced rats with BCP exhibited a pronounced

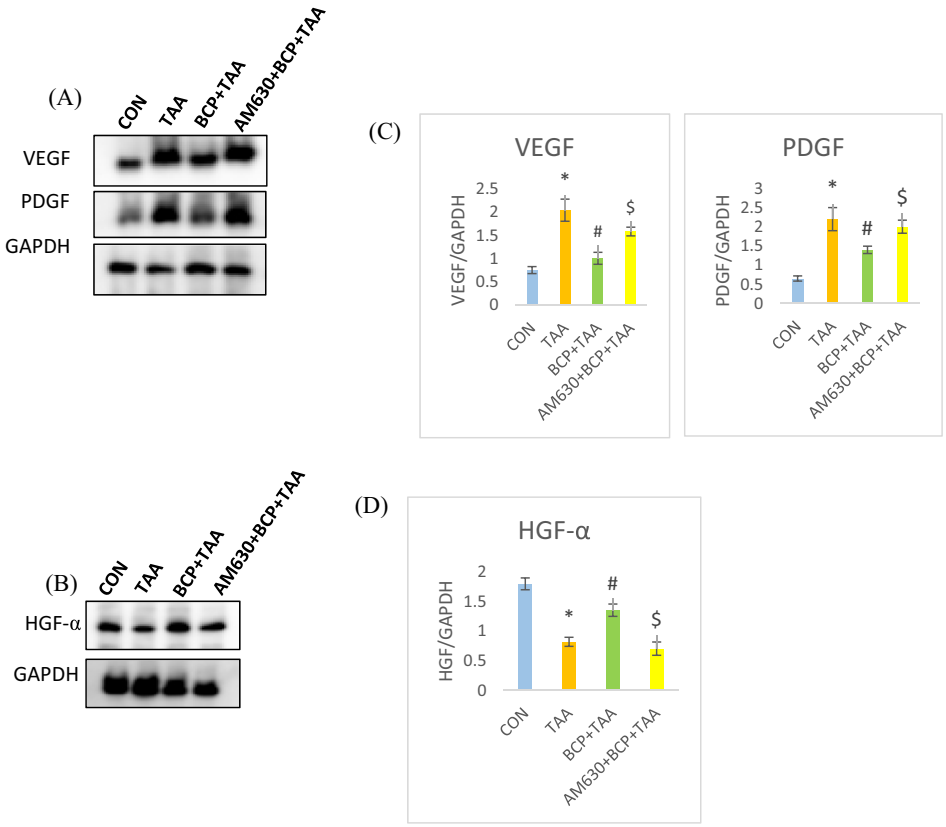

FIGURE 7 | Protein expression of VEGF, PDGF and HGF-α. Immunoblotting analysis of (A) VEGF and PDGF, (B) HGF-α. Protein expression quantification of (C) VEGF and PDGF, (D) HGF-α ($n = 3–4$). $^{*}p < 0.05$ CON vs. TAA, $^{\#}p < 0.05$ TAA vs. BCP + TAA, $^{\$}p < 0.05$ BCP + TAA vs. AM630 + BCP + TAA (one-way ANOVA followed by DMRT). CON: Control, BCP + TAA: β-Caryophyllene+ Thioacetamide treatment, AM630 + BCP + TAA: AM630 + β-Caryophyllene + Thioacetamide.

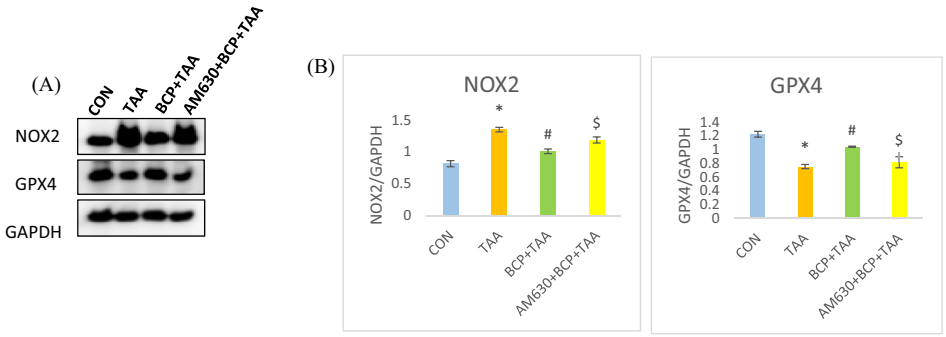

FIGURE 8 | Protein expression of NOX2 and GPX4. (A) Western blots of NOX2 and GPX4. (B) Quantification of NOX2 and GPX4 protein expression ($n = 3–4$). $^{*}p < 0.05$ CON vs. TAA, $^{\#}p < 0.05$ TAA vs. BCP + TAA, $^{\$}p < 0.05$ BCP + TAA vs. AM630 + BCP + TAA (one-way ANOVA followed by DMRT). CON: Control, BCP + TAA: β-Caryophyllene+ Thioacetamide treatment, AM630 + BCP + TAA: AM630 + β-Caryophyllene + Thioacetamide.

protection on the level of hepatic antioxidant enzymes. BCP reinstated redox balance, lowering NOX2 expression, while restoring GPX1 and GPX4 activities. This aligns with published findings showing BCP suppresses NOX2 activity and enhances GPX-dependent antioxidant capacity [31, 32]. Oxidative stress has a role in inducing and amplifying necroptosis. Generated ROS promotes autophosphorylation and activation of RIPK1 and the subsequent formation of necrosome through binding with RIPK3. Therefore, suppressing ROS production inhibits necroptosis induction [33].

In liver fibrosis, damaged hepatocytes undergo necroptosis, a regulated form of cell death, associated with an amplified inflammation due to the release of damage-associated molecular patterns from necroptotic cells. Necroptosis is mediated by RIPK1 and RIPK2 with the executioner protein MLKL. This type of cellular death is considered a driving mechanism of hepatocellular injury and fibrogenesis and a novel mode of cellular demise in various liver diseases such as nonalcoholic fatty liver disease (NAFLD) and nonalcoholic steatohepatitis (NASH) [34]. Inhibiting necroptotic mediators, such as blocking

RIPK1 activation and suppressing RIPK3 phosphorylation and MLKL membrane translocation, attenuates hepatic fibrosis, as proven in various experimental models [35–37]. TAA exposure induces the generation of ROS, release of cytokines, and activation of death receptors, all of which converge on stimulating the necroptosis pathway. In our study, TAA administration markedly increased the expression of necroptotic markers; RIPK1, RIPK3 and p-MLKL, indicating activated necroptotic cell death in fibrotic liver. This aligns with other studies showing RIPK1/RIPK3/p-MLKL signaling as a key driving force of fibrosis in other hepatic disease models [38]. Notably, BCP treatment suppressed the RIPK1/RIPK3/p-MLKL axis, evident in their downregulated expression, thereby limiting hepatocyte death.

CB2 receptor is a Gi/o-coupled G protein coupled receptor (GPCR), a signaling molecule that can inhibit adenylate cyclase and modulate several signaling cascades intracellularly [39]. Activation of CB2 receptors is correlated to the inhibition of necroptosis through various mechanisms. CB2 receptors inhibit the upstream signaling which ultimately suppresses necroptosis induction. CB2 receptors' signaling blocks the production of the inflammatory cytokine TNF-α, thereby abrogating TNFR1-mediated stimulation of RIPK1–RIPK3 necrosome formation and necroptosis initiation [40]. In addition, activated CB2 receptors favor an anti-inflammatory environment. The decreased cAMP due to inhibited adenylyl cyclase enzyme suppresses PKA, and thus inhibits the phosphorylation of the 65 subunit and prevents NF-κB nuclear translocation [41]. This allows shifting toward pro-survival and promotes RIPK1 ubiquitination, preventing its transition into pro-necroptotic complexes. It is also reported that attenuated oxidative stress is linked to weakened RIPK1/RIPK3 signaling and thereby less MLKL activation and membrane permeabilization [42].

Platelet derived growth factor (PDGF) and vascular endothelial growth factor (VEGF) are profibrogenic mediators involved in the initiation of liver fibrosis. PDGF is a potent mitogen that induces the activation, proliferation, and migration of HSC, thereby accelerating ECM deposition [43]. Similarly, VEGF promotes pathological angiogenesis, which enhances HSC activation and sustains the inflammatory response and therefore contributes to fibrogenesis. PDGF also plays a role in vascular stabilization and promotes maturation of new blood vessels [44]. Our study demonstrated that the administration of TAA markedly increased hepatic expression of both PDGF and VEGF, promoting angiogenic signaling during fibrosis development. Other studies also reported increased hepatic VEGF and PDGF following TAA exposure [45, 46]. Administered BCP reduced the upregulated level of PDGF and VEGF, suppressing angiogenic pathways. Although the data on BCP effect on PDGF and VEGF within hepatic tissue remain scarce, its regulatory effects on these mediators have been reported in several non-hepatic models [47]. Both PDGF and VEGF have pro-fibrogenic effects; however, hepatocyte growth factor (HGF-α) is a key anti-fibrotic mediator with hepatoprotective effects. HGF-α is an endogenous mediator that promotes liver reaeration and opposes fibrogenesis by stimulating hepatocyte proliferation, suppressing stellate cells transdifferentiation, and downregulating TGF-β. During chronic liver injury, HGF-α levels decline, which impairs the liver's ability to repair itself [48]. Therefore, enhancing HGF-α signaling is valuable in counteracting fibrosis. Consistent with this concept, our findings demonstrate that BCP treatment increased HGF-α levels, reinforcing the liver's intrinsic regenerative mechanisms. Compounds with pro-regenerative actions have been shown to counteract TAA-induced suppression of liver regenerative capacity, supporting the therapeutic value of restoring regenerative pathways [49].

AM630 is widely used as a pharmacological tool to investigate CB2-mediated actions. The use of AM630 as a selective antagonist has been reported in various liver-disease models [22, 50] and has also been co-administered with BCP in non-hepatic models to confirm CB2-dependent actions [51, 52]. In our study, the co-administration of AM630 completely shifted the picture of BCP protective effects. In our results, AM630 abolished the beneficial effects of BCP on all evaluated parameters, including liver function, fibrosis, inflammation, oxidative stress, and necroptosis. While BCP alone markedly improved serum functional markers and liver index, decreased pro-inflammatory mediators, restored antioxidant defense, mitigated fibrotic and angiogenic markers, and suppressed the necroptosis cascade, these effects were lost when BCP was administered with AM630. Oxidative stress indices, fibrotic markers, and necroptotic proteins reverted toward TAA-group values, indicating that AM630 effectively counteracted BCP hepatoprotection. This reversal of BCP actions suggests that BCP's effects are critically dependent on CB2 receptors activation. Given that CB2 receptors are expressed on hepatic stellate cells, Kupffer cells, and other non-parenchymal cells involved in inflammation and fibrogenesis, the blockade of these receptors by AM630 inhibits BCP modulatory effects. Taken together, our findings strongly support that the hepatoprotective effects of BCP in TAA-induced fibrosis are CB2 receptors-dependent. Although an AM630-alone group was not included in the present study, this experimental condition was evaluated in our previous work [24] using the same model and treatment protocol, where AM630 administration alone did not significantly affect the assessed hepatic parameters. Consequently, the current study focused on investigating the ability of AM630 to modulate the effects of BCP and thereby clarify the involvement of CB2 receptor signaling. Furthermore, the omission of an additional AM630-only group helped avoid unnecessary repetition of experiments and reduced animal use in accordance with established ethical principles.

As explained in our previous publication [24], this study was exclusively conducted on male rats to minimize the hormonal variability associated with the estrous cycle in female rats, which is associated with significant fluctuations in estrogen, a hormone known to play a role in liver fibrosis development and progression. The exclusion of female rats was intended to provide a consistent and established baseline model for liver fibrosis that excludes confounding factors, such as the hormonal variability observed in females. Given the fact that hormonal influence is temporary and eliminated with menopause, at which the risk of liver fibrosis becomes equivalent to the risk for males [53].

The findings of the present study should be interpreted in the context of our previous publication [24] investigating the preventive effects of β-caryophyllene (BCP) in TAA-induced liver fibrosis. In the earlier study, BCP administration was initiated concurrently with TAA exposure, thereby evaluating its ability to prevent or attenuate the development of hepatic injury and

fibrosis. In contrast, the present study employed a therapeutic intervention design, in which BCP treatment was initiated after 6 weeks of TAA administration, when liver injury and fibrotic changes had already been established. Consequently, the current investigation addresses a distinct and more clinically relevant question regarding the capacity of BCP to mitigate ongoing hepatic damage rather than prevent disease initiation. Therefore, the present work extends our earlier findings by providing evidence that BCP may exert beneficial effects not only during fibrosis development but also after disease establishment. Collectively, these findings provide preclinical evidence supporting the potential of BCP as an experimental antifibrotic intervention; however, further pharmacokinetic, toxicological, and clinical studies are required before its therapeutic applicability can be established.

5 | Conclusion

The present study demonstrates that TAA induces profound hepatic damage, manifested by intense oxidative and inflammatory response, pronounced necroptotic death and activated fibrosis. Treatment with BCP countered these pathological alterations and restored biochemical and histological integrity through its anti-inflammatory, antioxidant, and anti-fibrotic properties. In addition to mitigating liver injury, BCP enhances liver's recovery through promoting regenerative signaling. The concurrent administration of AM630 abolished these beneficial effects across all assessed parameters, highlighting the CB2 receptors-related mechanistic dependability. Collectively, these findings provide insight into the multifaceted mechanisms implicated in BCP's therapeutic potential and position CB2 receptor signaling as a promising target for combating liver fibrosis. The present study provides a novel mechanistic insight into the effect of BCP on necroptosis. This study adds to the literature by delineating the modulation of necroptotic cellular death and RIPK1/RIPK3/MLKL signaling axis by BCP. These findings advance our understanding beyond the well-reported anti-inflammatory and antioxidant effects of BCP and identify necroptosis as a new target of it. Thus, this elucidates a new dimension in BCP therapeutic mechanisms. Further future studies are warranted to decipher its translational relevance and therapeutic applicability as the study solely relied on chemically induced liver fibrosis which may not fully capture the complexity of human liver fibrosis. Additionally, genetic confirmation using CB2 knockout models would strengthen the causal involvement of CB2 receptors in BCP-exerted effects.

Author Contributions

Loay Lubbad: methodology, data curation. **Fayez T. Hammad:** methodology, resources. **Seenipandi Arunachalam:** methodology. **Ernest Adeghate:** validation, data curation. **Sandeep Subramanya:** data curation, validation. **Lujain Bader Eddin:** writing – original draft, methodology, investigation, data analysis, validation, writing – review and editing, data curation. **Shreesh Ojha:** conceptualization, supervision, project administration, funding acquisition, validation.

Acknowledgments

The authors are thankful to the United Arab Emirates University for the award of the research grants (#12R121 to Shreesh Ojha).

Conflicts of Interest

The authors declare no conflicts of interest.

Data Availability Statement

The data that support the findings of this study are available from the corresponding author upon reasonable request.

References

1. A. Treyer and A. Müsch, "Hepatocyte Polarity," *Comprehensive Physiology* 3 (2013): 243–287, https://doi.org/10.1002/cphy.c120009.

2. R. Bataller and D. A. Brenner, "Liver Fibrosis," *Journal of Clinical Investigation* 115 (2005): 209–218, https://doi.org/10.1172/jci24282.

3. Y. Liu, T. Liu, T. Lei, et al., "RIP1/RIP3-Regulated Necroptosis as a Target for Multifaceted Disease Therapy (Review)," *International Journal of Molecular Medicine* 44 (2019): 771–786, https://doi.org/10.3892/ijmm.2019.4244.

4. M. B. Afonso, P. M. Rodrigues, T. Carvalho, et al., "Necroptosis Is a Key Pathogenic Event in Human and Experimental Murine Models of Non-Alcoholic Steatohepatitis," *Clinical Science (London)* 129 (2015): 721–739, https://doi.org/10.1042/cs20140732.

5. A. Majdi, L. Aoudjehane, V. Ratziu, et al., "Inhibition of Receptor-Interacting Protein Kinase 1 Improves Experimental Non-Alcoholic Fatty Liver Disease," *Journal of Hepatology* 72 (2020): 627–635, https://doi.org/10.1016/j.jhep.2019.11.008.

6. M. B. Afonso, P. M. Rodrigues, M. Mateus-Pinheiro, et al., "RIPK3 Acts as a Lipid Metabolism Regulator Contributing to Inflammation and Carcinogenesis in Non-Alcoholic Fatty Liver Disease," *Gut* 70 (2021): 2359–2372, https://doi.org/10.1136/gutjnl-2020-321767.

7. F. Zhan, G. Zhao, X. Li, et al., "Inositol-Requiring Enzyme 1 Alpha Endoribonuclease Specific Inhibitor STF-083010 Protects the Liver From Thioacetamide-Induced Oxidative Stress, Inflammation and Injury by Triggering Hepatocyte Autophagy," *International Immunopharmacology* 73 (2019): 261–269, https://doi.org/10.1016/j.intimp.2019.04.051.

8. Z. Loh, R. L. Fitzsimmons, R. C. Reid, et al., "Inhibitors of Class I Histone Deacetylases Attenuate Thioacetamide-Induced Liver Fibrosis in Mice by Suppressing Hepatic Type 2 Inflammation," *British Journal of Pharmacology* 176 (2019): 3775–3790, https://doi.org/10.1111/bph.14768.

9. J. Chilakapati, K. Shankar, M. C. Korrapati, R. A. Hill, and H. M. Mehendale, "Saturation Toxicokinetics of Thioacetamide: Role in Initiation of Liver Injury," *Drug Metabolism and Disposition* 33 (2005): 1877–1885, https://doi.org/10.1124/dmd.105.005520.

10. E. B. Russo, "Taming THC: Potential Cannabis Synergy and Phytocannabinoid-Terpenoid Entourage Effects," *British Journal of Pharmacology* 163 (2011): 1344–1364, https://doi.org/10.1111/j.1476-5381.2011.01238.x.

11. J. Gertsch, M. Leonti, S. Raduner, et al., "Beta-Caryophyllene Is a Dietary Cannabinoid," *Proceedings of the National Academy of Sciences of the United States of America* 105 (2008): 9099–9104, https://doi.org/10.1073/pnas.0803601105.

12. M. Ennajar, J. Bouajila, A. Lebrihi, et al., "Chemical Composition and Antimicrobial and Antioxidant Activities of Essential Oils and Various Extracts of *Juniperus phoenicea* L. (Cupressacees)," *Journal of Food Science* 74 (2009): M364–M371, https://doi.org/10.1111/j.1750-3841.2009.01277.x.

13. R. Scandiffio, F. Geddo, E. Cottone, et al., "Protective Effects of (E)-β-Caryophyllene (BCP) in Chronic Inflammation," *Nutrients* 12 (2020): 3273, https://doi.org/10.3390/nu12113273.

14. J. Tchekalarova, K. da Conceição Machado, A. L. Gomes Júnior, A. A. de Carvalho Melo Cavalcante, A. Momchilova, and R. Tzoneva,

"Pharmacological Characterization of the Cannabinoid Receptor 2 Agonist, β-Caryophyllene on Seizure Models in Mice," *Seizure* 57 (2018): 22–26, https://doi.org/10.1016/j.seizure.2018.03.009.

15. M. F. N. Meeran, F. Laham, S. Azimullah, et al., "β-Caryophyllene, a Natural Bicyclic Sesquiterpene Attenuates β-Adrenergic Agonist-Induced Myocardial Injury in a Cannabinoid Receptor-2 Dependent and Independent Manner," *Free Radical Biology & Medicine* 167 (2021): 348–366, https://doi.org/10.1016/j.freeradbiomed.2021.01.046.

16. A. M. Al-Attar and H. A. Al-Rethea, "Chemoprotective Effect of Omega-3 Fatty Acids on Thioacetamide Induced Hepatic Fibrosis in Male Rats," *Saudi Journal of Biological Sciences* 24 (2017): 956–965, https://doi.org/10.1016/j.sjbs.2016.01.029.

17. Z. V. Varga, C. Matyas, K. Erdelyi, et al., "β-Caryophyllene Protects Against Alcoholic Steatohepatitis by Attenuating Inflammation and Metabolic Dysregulation in Mice," *British Journal of Pharmacology* 175 (2018): 320–334, https://doi.org/10.1111/bph.13722.

18. A. A. Harb, Y. K. Bustanji, and S. S. Abdalla, "Hypocholesterolemic Effect of β-Caryophyllene in Rats Fed Cholesterol and Fat Enriched Diet," *Journal of Clinical Biochemistry and Nutrition* 62 (2018): 230–237, https://doi.org/10.3164/jcbn.17-3.

19. T. Tsuchida and S. L. Friedman, "Mechanisms of Hepatic Stellate Cell Activation," *Nature Reviews. Gastroenterology & Hepatology* 14 (2017): 397–411, https://doi.org/10.1038/nrgastro.2017.38.

20. B. Dewidar, J. Soukupova, I. Fabregat, and S. Dooley, "TGF-β in Hepatic Stellate Cell Activation and Liver Fibrogenesis: Updated," *Current Pathobiology Reports* 3 (2015): 291–305, https://doi.org/10.1007/s40139-015-0089-8.

21. X. Zhou, L. Yu, M. Zhou, P. Hou, L. Yi, and M. Mi, "Dihydromyricetin Ameliorates Liver Fibrosis via Inhibition of Hepatic Stellate Cells by Inducing Autophagy and Natural Killer Cell-Mediated Killing Effect," *Nutrition & Metabolism (London)* 18 (2021): 64, https://doi.org/10.1186/s12986-021-00589-6.

22. M. F. Mahmoud, S. E. Swefy, R. A. Hasan, and A. Ibrahim, "Role of Cannabinoid Receptors in Hepatic Fibrosis and Apoptosis Associated With Bile Duct Ligation in Rats," *European Journal of Pharmacology* 742 (2014): 118–124, https://doi.org/10.1016/j.ejphar.2014.08.021.

23. N. Arizuka, T. Murakami, and K. Suzuki, "The Effect of β-Caryophyllene on Nonalcoholic Steatohepatitis," *Journal of Toxicologic Pathology* 30 (2017): 263–273, https://doi.org/10.1293/tox.2017-0018.

24. L. Bader Eddin, A. Mahgoub, S. Almarzooqi, E. Adeghate, S. B. Subramanya, and S. Ojha, "β-Caryophyllene Ameliorates Thioacetamide-Induced Liver Fibrosis in Rats: A Preventative Approach," *International Journal of Molecular Sciences* 26 (2025): 8493, https://doi.org/10.3390/ijms26178493.

25. S. T. Elazab and R. E. A. G. Eldin, "α-Bisabolol and Royal Jelly Differentially Mitigate Thioacetamide-Induced Hepatic Fibrosis in Rats Associated With the Inhibition of TGF-β1/FAK/α-SMA Signaling," *Food and Chemical Toxicology* 193 (2024): 115069, https://doi.org/10.1016/j.fct.2024.115069.

26. L. Hammerich and F. Tacke, "Hepatic Inflammatory Responses in Liver Fibrosis," *Nature Reviews. Gastroenterology & Hepatology* 20 (2023): 633–646, https://doi.org/10.1038/s41575-023-00807-x.

27. T. Y. Lee, H. H. Chang, C. K. Wen, T. H. Huang, and Y. S. Chang, "Modulation of Thioacetamide-Induced Hepatic Inflammations, Angiogenesis and Fibrosis by Andrographolide in Mice," *Journal of Ethnopharmacology* 158, no. Pt A (2014): 423–430, https://doi.org/10.1016/j.jep.2014.10.056.

28. Y. Zhao, X. Liu, C. Ding, Y. Gu, and W. Liu, "Dihydromyricetin Reverses Thioacetamide-Induced Liver Fibrosis Through Inhibiting NF-κB-Mediated Inflammation and TGF-β1-Regulated of PI3K/Akt Signaling Pathway," *Frontiers in Pharmacology* 12 (2021): 783886.

29. A. Allameh, R. Niayesh-Mehr, A. Aliarab, G. Sebastiani, and K. Pantopoulos, "Oxidative Stress in Liver Pathophysiology and Disease," *Antioxidants (Basel)* 12 (2023): 1653, https://doi.org/10.3390/antiox12091653.

30. A. Albrakati, "Protective Effects of Shikimic Acid Against Thioacetamide-Induced Hepatic Fibrosis: Role of Nrf2/NF-κB Signaling Pathways," *Frontiers in Pharmacology* 16 (2025): 1609711.

31. H. Li, D. Wang, Y. Chen, and M. Yang, "β-Caryophyllene Inhibits High Glucose-Induced Oxidative Stress, Inflammation and Extracellular Matrix Accumulation in Mesangial Cells," *International Immunopharmacology* 84 (2020): 106556, https://doi.org/10.1016/j.intimp.2020.106556.

32. Y. Li, W. Wu, Y. Song, et al., "β-Caryophyllene Confers Cardioprotection by Scavenging Radicals and Blocking Ferroptosis," *Journal of Agricultural and Food Chemistry* 72 (2024): 18003–18012, https://doi.org/10.1021/acs.jafc.4c03239.

33. S. Xian, Y. Yang, N. Nan, et al., "Inhibition of Mitochondrial ROS-Mediated Necroptosis by Dendrobium Nobile Lindl. Alkaloids in Carbon Tetrachloride Induced Acute Liver Injury," *Journal of Ethnopharmacology* 330 (2024): 118253, https://doi.org/10.1016/j.jep.2024.118253.

34. W. K. Saeed and D. W. Jun, "Necroptosis: An Emerging Type of Cell Death in Liver Diseases," *World Journal of Gastroenterology* 20 (2014): 12526–12532, https://doi.org/10.3748/wjg.v20.i35.12526.

35. Y. Yi, W. Zhang, L. Tao, et al., "RIP1 Kinase Inactivation Protects Against Acetaminophen-Induced Acute Liver Injury in Mice," *Free Radical Biology & Medicine* 174 (2021): 57–65, https://doi.org/10.1016/j.freeradbiomed.2021.07.034.

36. A. Li, D. Chen, and J. Shen, "Inhibition RIP1 Prevents Acute Liver Failure by Suppressing Hepatic Apoptosis and Attenuating the Secretion of TNF-α From Macrophages," *European Journal of Medical Research* 30 (2025): 675, https://doi.org/10.1186/s40001-025-02948-y.

37. S. Wei, H. Zhou, Q. Wang, et al., "RIP3 Deficiency Alleviates Liver Fibrosis by Inhibiting ROCK1-TLR4-NF-κB Pathway in Macrophages," *FASEB Journal* 33 (2019): 11180–11193, https://doi.org/10.1096/fj.201900752R.

38. X. Wu, R. K. Arya, E. Huang, M. R. McMullen, and L. E. Nagy, "Receptor-Interacting Protein 1 and 3 Kinase Activity Are Required for High-Fat Diet Induced Liver Injury in Mice," *Frontiers in Endocrinology* 14 (2023): 1267996.

39. G. D. Dalton, C. E. Bass, C. G. Van Horn, and A. C. Howlett, "Signal Transduction via Cannabinoid Receptors," *CNS & Neurological Disorders Drug Targets* 8 (2009): 422–431, https://doi.org/10.2174/187152709789824615.

40. A. Capozzi, D. Caissutti, V. Mattei, et al., "Anti-Inflammatory Activity of a CB2 Selective Cannabinoid Receptor Agonist: Signaling and Cytokines Release in Blood Mononuclear Cells," *Molecules* 27 (2022): 64, https://doi.org/10.3390/molecules27010064.

41. S. Gerlo, R. Kooijman, I. M. Beck, K. Kolmus, A. Spooren, and G. Haegeman, "Cyclic AMP: A Selective Modulator of NF-κB Action," *Cellular and Molecular Life Sciences* 68 (2011): 3823–3841, https://doi.org/10.1007/s00018-011-0757-8.

42. Y. Zhang, S. S. Su, S. Zhao, et al., "RIP1 Autophosphorylation Is Promoted by Mitochondrial ROS and Is Essential for RIP3 Recruitment Into Necrosome," *Nature Communications* 8 (2017): 14329, https://doi.org/10.1038/ncomms14329.

43. H. Z. Ying, Q. Chen, W. Y. Zhang, et al., "PDGF Signaling Pathway in Hepatic Fibrosis Pathogenesis and Therapeutics (Review)," *Molecular Medicine Reports* 16 (2017): 7879–7889, https://doi.org/10.3892/mmr.2017.7641.

44. M. Mejias, A. Balvey, and M. Fernandez, "Crosstalk Between Angiogenesis and Fibrogenesis in Liver Disease," *Current Tissue*

Microenvironment Reports 1 (2020): 121–129, https://doi.org/10.1007/s43152-020-00013-w.

45. A. A. Elnfarawy, A. E. Nashy, A. M. Abozaid, I. F. Komber, R. H. Elweshahy, and R. S. Abdelrahman, "Vinpocetine Attenuates Thioacetamide-Induced Liver Fibrosis in Rats," *Human & Experimental Toxicology* 40 (2021): 355–368, https://doi.org/10.1177/0960327120947453.

46. R. Salguero Palacios, M. Roderfeld, S. Hemmann, et al., "Activation of Hepatic Stellate Cells Is Associated With Cytokine Expression in Thioacetamide-Induced Hepatic Fibrosis in Mice," *Laboratory Investigation* 88 (2008): 1192–1203, https://doi.org/10.1038/labinvest.2008.91.

47. F. Wittig, F. Koch, L. Pannenberg, S. Bekeschus, R. Ramer, and B. Hinz, "β-Caryophyllene Inhibits Endothelial Tube Formation by Modulating the Secretome of Hypoxic Lung Cancer Cells—Possible Role of VEGF Downregulation," *International Journal of Molecular Sciences* 25 (2024): 810, https://doi.org/10.3390/ijms25020810.

48. Y. Zhao, W. Ye, Y.-D. Wang, and W.-D. Chen, "HGF/c-Met: A Key Promoter in Liver Regeneration," *Frontiers in Pharmacology* 13 (2022): 808855.

49. A. M. H. Ghanim, N. S. Younis, and H. A. Metwaly, "Vanillin Augments Liver Regeneration Effectively in Thioacetamide Induced Liver Fibrosis Rat Model," *Life Sciences* 286 (2021): 120036, https://doi.org/10.1016/j.lfs.2021.120036.

50. H. C. Huang, S. S. Wang, I. F. Hsin, et al., "Cannabinoid Receptor 2 Agonist Ameliorates Mesenteric Angiogenesis and Portosystemic Collaterals in Cirrhotic Rats," *Hepatology* 56 (2012): 248–258, https://doi.org/10.1002/hep.25625.

51. A. F. Bento, R. Marcon, R. C. Dutra, et al., "β-Caryophyllene Inhibits Dextran Sulfate Sodium-Induced Colitis in Mice Through CB2 Receptor Activation and PPARγ Pathway," *American Journal of Pathology* 178 (2011): 1153–1166, https://doi.org/10.1016/j.ajpath.2010.11.052.

52. A. M. Bagher, "Intraplantar β-Caryophyllene Alleviates Pain and Inflammation in STZ-Induced Diabetic Peripheral Neuropathy via CB(2) Receptor Activation," *International Journal of Molecular Sciences* 26 (2025): 4430, https://doi.org/10.3390/ijms26094430.

53. J. D. Yang, M. F. Abdelmalek, H. Pang, et al., "Gender and Menopause Impact Severity of Fibrosis Among Patients With Nonalcoholic Steatohepatitis," *Hepatology* 59 (2014): 1406–1414, https://doi.org/10.1002/hep.26761.